Current Balance at the Surface of a Cold Cathode

D. A. Doughty, E. A. Den Hartog, and J. E. Lawler
Department of Physics, University of Wisconsin, Madison, Wisconsin 53706
(Received 9 February 1987)

Recent experimental and theoretical developments, including an electric field diagnostic based on optogalvanic detection of Rydberg atoms, an analytic treatment of ion transport in the cathode fall, and a null collision Monte Carlo technique, are combined to determine the current balance at the surface of a cold cathode in a He glow discharge. The ratio of the ion current to electron current is measured and calculated over a range of current densities from a near-normal to a highly abnormal glow discharge.

PACS numbers: 52.80.Hc, 51.10.+y, 52.20.Fs, 52.20.Hv

New experimental diagnostics and recent theoretical developments are leading to a more quantitative understanding of the cathode-fall region of the glow discharge. The development of detailed quantitative models has been hampered by the nonequilibrium nature of the cathode-fall region. The proximity of the boundary and the large spatial variation of the electric field give rise to an electron distribution function that is not in hydrodynamic equilibrium with the local electric field to gas density ratio (E/N). Therefore, the large data base of electron transport parameters is not directly applicable when modeling the cathode fall. Although the cathode-fall region is the least understood part of a typical discharge, this region is very important from a practical and a fundamental viewpoint.

We measure the current balance at the cathode surface by utilizing an electric field diagnostic and a Boltzmann-equation analysis of ion transport. Spatially resolved electric fields can be measured with either laser-induced fluorescence[1] or optogalvanic detection of Rydberg atoms.[2,3] The latter technique is the most suitable for the discharge studied in this work. The spatial gradient of the electric field determines the space-charge density by Poisson's equation. This space-charge density is almost entirely due to ions since the electron density is negligible in the high electric fields of the cathode-fall region. The ion current density is simply the product of the ion charge density and the average ion velocity.

Analytic nonequilibrium solutions to the Boltzmann equation for ions were used to calculate the equilibration distance of ions in the cathode fall.[4] The calculations included the symmetric-charge-exchange term, a nonuniform field, and a distributed-ion-source term. The average ion velocity is the equilibrium drift velocity for ions more than six mean free paths from the cathode-fall–negative-glow boundary.[4] The cathode fall has a thickness of sixty mean free paths for symmetric charge exchange; thus the equilibrium drift velocity can be used to calculate the ion current density. The difference between the measured total current density and this ion current density is the electron current density. The ratio of the ion-to-electron current at the cathode surface can be directly compared to a suitable calculation. We use a Monte Carlo code based on a null collision technique to simulate electron avalanches in the cathode fall.[5-7] The average number of ions produced per electron emitted from the cathode in these simulations compares favorably to the empirical ion-to-electron–current ratio.

This "electric field" approach is used to determine the current balance at a cold Al cathode in a 3.5-Torr He discharge over a range of discharge current densities from 0.190 to 1.50 mA/cm^2. The current-density range extends from a near-normal cathode-fall voltage of 173 V to a highly abnormal cathode-fall voltage of 600 V. We find that the ratio of ion current to electron current at the cathode is approximately 3.3 over the entire range.

The discharge is produced between flat circular Al electrodes 3.2 cm in diameter and separated by 0.62 cm. The discharge tube is made primarily of glass and stainless steel. Most of the large seals are made with knife-edge flanges on Cu gaskets. The only exceptions are the high-vacuum epoxy seals around the fused silica Brewster windows. A liquid-N_2 trapped diffusion pump evacuates the tube to 2×10^{-8} Torr. When no liquid N_2 is in the trap an ion pump maintains the vacuum to prevent oil from backdiffusing into the system. The leak rate into the discharge tube is approximately 3×10^{-4} Torr/d. For discharge operations ultrahigh-purity (0.99999) He is slowly flowed through the system. A capacitive manometer monitors the pressure, which is maintained at 3.5 Torr. The He first passes through a cataphoresis discharge to remove any residual contaminants before entering the main discharge tube. Emission spectra reveal only very weak Al and H impurity lines. In order to perform spatially resolved measurements without disturbing laser alignment the discharge is mounted on a precision translation stage. Optogalvanic effects are detected as a change in discharge current with a boxcar averager. The appropriate laser radiation is produced with a N_2-laser–pumped dye-laser system which has a bandwidth of 0.4 cm^{-1}. For electric field measurements the dye laser is frequency doubled. The second harmonic is polarized normal to the surface of the electrodes and is focused with a cylindrical lens to a strip 0.01 cm wide

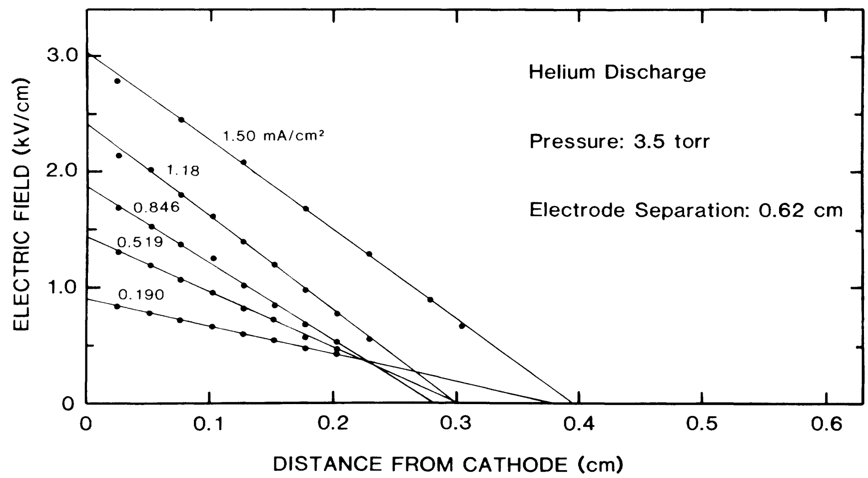

FIG. 1. Electric field as a function of distance from the cathode for the five currents studied. The anode corresponds to the right-hand side of the figure.

and 1 cm long parallel to the electrode surface. Schematics of the apparatus are presented in previous publications.[2,3]

The electric field in the cathode-fall region is mapped by the observing of atomic transitions from heavily populated metastable levels to Rydberg levels. Optogalvanic detection is essential because the fragile Rydberg atoms are collisionally ionized in the discharge long before they can fluoresce. These transitions exhibit a dramatic linear Stark effect because of the large size of Rydberg atoms and because of the small energy gap between states of opposite parity. To interpret Stark spectra a $n \times n$ (n is the principal quantum number) Hamiltonian matrix is diagonalized yielding eigenvalues which are the perturbed energies of the states in the Stark manifold.[8] The eigenvectors can be related to the intensities of the various components in the Stark manifold. Stark spectra are obtained by scanning the frequency of the laser in a fixed spatial position. The width of the Stark manifold, the separation of individual components, or the relative intensities of the components can each be used to determine the field. The 2^1S to 11^1P transition in He at 321 nm is well suited for measuring fields found in low-pressure discharges. The width of the Stark manifold increases as n^2; thus the optimum n is determined by the magnitude of the fields being studied.

The electric field measurements are summarized in Fig. 1 and Table I for the five discharge current densities, J_D. Figure 1 is a plot of electric field as a function of distance away from the cathode. The solid lines are linear fits to the data. This linear behavior persists to very small fields.[9] Table I lists the electric fields at the cathode, E^0, and the zero-field positions, d_c, which are determined by linearly extrapolating the data. The boundary between the cathode-fall and negative-glow regions is confirmed by a change in magnitude and temporal characteristics of optogalvanic effects at a distance d_c from the surface of the cathode. The excellent agreement between $V_{\rm ef}$, a voltage determined by integrating the field data, and $V_{\rm vm}$, a voltage measured with a digital voltmeter, indicates that the field measurements are on the average accurate to 1%.

The discharge electrodes are water cooled in order to minimize gas heating in the cathode fall. This cooling does not completely eliminate a temperature increase and subsequent density reduction in the abnormal glow. Symmetric charge exchange between positive ions and neutrals converts over half of the input power to heavy-particle translational motion in the cathode fall. The resulting temperature increase is measured from the

TABLE I. Experimentally determined parameters.

J_D (mA/cm^2)	E^0 (V/cm)	d_c (cm)	$V_{\rm vm}$ (V)	$V_{\rm ef}$ (V)	N (10^{16} cm^{-3})	ρ_+ (10^{-10} C/cm^3)	U^0_+ (10^5 cm/s)	J^0_+ (mA/cm^2)
1.50	3017	0.396	600	597	8.01	6.74	16.5	1.11
1.18	2395	0.300	356	359	9.48	7.07	13.2	0.933
0.846	1870	0.282	261	264	10.3	5.88	10.9	0.641
0.519	1426	0.301	211	215	10.8	4.20	9.28	0.390
0.190	897	0.382	173	171	11.2	2.08	7.12	0.148

Doppler width of the 2^1S to 3^1P transition in He at 501.6 nm. An étalon reduces the dye-laser bandwidth to 300 MHz for the Doppler-width measurements which are made by optogalvanic detection. The 501.6-nm transition has a natural width of 92 MHz.[10] Pressure broadening at 3.5 Torr contributes another 146 MHz.[11] Stark broadening adds at most a few hundred megahertz. These contributions are all much smaller than the Doppler width of 3.66 GHz at room temperature. The column labeled N in Table I is the resulting gas-density measurements. The uncertainty ranges from $\pm 3\%$ at low currents to $\pm 6\%$ at the high currents. The gas density is constant throughout the cathode-fall region to within the 3%–6% uncertainty of the measurements.

The ion current density at the surface of the cathode is the product of the ion density, ρ_+, and the ion drift velocity at the cathode surface, U_+^0. Poisson's equation combined with the electric field data gives the ion density. The uncertainty in ρ_+ is comparable to the uncertainty in the field measurements. To determine the drift velocity at low currents Helm's precise mobility data are used.[12] At the high currents the drift velocity is calculated with use of the equilibrium expression,

$$U_+^0 = (2eE^0/M\pi\sigma N)^{1/2}, \tag{1}$$

where e is the ion charge and M the ion mass. The symmetric-charge-exchange cross section, σ, is taken from the calculations of Sinha, Lin, and Bardsley.[13] These calculations agree with Helm's experimentally derived cross sections. The uncertainty in U_+^0 is $\pm 4\%$ in all cases. The ion current density at the cathode surface, J_+^0, is listed in the last column of Table I.

A Monte Carlo code is used to study electron avalanches in the cathode-fall region. Empirical fields and gas densities from Table I are used in the simulations. The position and momentum of individual electrons are followed in a Monte Carlo simulation. The code is based on an adaptation of the null collision technique for nonuniform fields.[5-7] In this approach a null collision cross section is chosen in order to avoid any numerical integration of collision probabilities along an electron's trajectory. The distance between collisions is determined by a random number, and the type of collision is determined by a second random number. If a null collision occurs, the electrons motion is unaffected. We use a code which includes anisotropic elastic scattering, excitation to 24 levels, direct ionization, and other less important processes. We choose the same set of elastic and inelastic cross sections used by Boeuf and Marode.[7,14,15] The Monte Carlo code with these cross sections is tested with use of a uniform E/N of 100 Td [1 Td (townsend) $= 10^{-17}$ V cm^2]. The simulation gives an equilibrium townsend coefficient that agrees with experiment. Figure 2 is a histogram of the ionization events per emitted electron as a function of distance from the cathode. This ionization peaks at the boundary between the cathode fall and the negative glow indicated by d_c. The nonequilibrium behavior of the electrons is evident from the large amount of ionization beyond d_c. If all the electrons in the negative glow were in equilibrium, they would produce very little ionization because the local field is small.

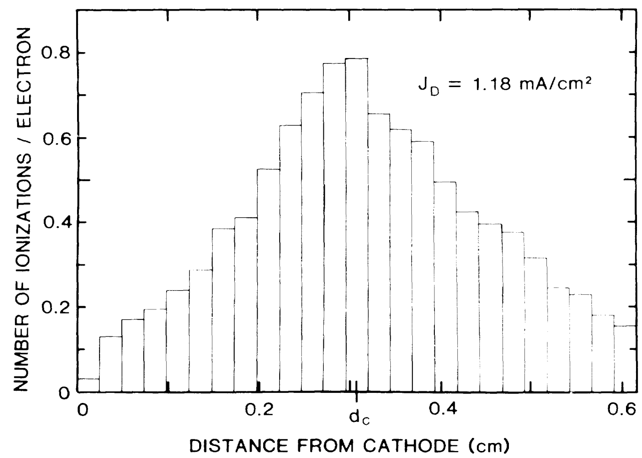

FIG. 2. Typical Monte Carlo histogram giving the total number of ionization events per electron released from the cathode as a function of distance from the cathode. Only those events between 0 and d_c are counted when evaluating the average size of an avalanche.

Although we have not been able to map the negative-glow field, we have evidence for a high density of low-energy electrons which indicates a very small (< 10 V/cm) field. We measure, using laser-induced fluorescence, a significant suppression of the 2^1S versus 2^3S metastable density in the negative-glow region. Our Monte Carlo simulations indicate only slight differences in the spatial dependence of the 2^1S and 2^3S production. The suppression is due to the reaction

$$\mathrm{He}(2^1S) + e^- + \mathrm{He}(2^3S) + e^- + 0.79\ \mathrm{eV}. \tag{2}$$

These observations indicate an electron temperature much less than 0.8 eV; otherwise the reaction would readily proceed in the opposite direction. Furthermore, an electron density of from 10^{12} to 10^{13} cm^{-3} in the negative glow can be inferred from these observations, because the rate of reaction (2) must overwhelm 2^1S metastable diffusion.[16,17]

Only ionization produced in the region to the left of d_c contributes to the ion current in the cathode fall. If the ions from the negative glow contributed to the cathode-fall current in a significant way then there must be a large ion current towards the cathode at d_c. Equation (1) indicates, however, a relatively small ion velocity because of the weak fields near the cathode-fall–negative-glow boundary. In fact Eq. (1) overestimates the average ion velocity near the negative glow.[4] Since the

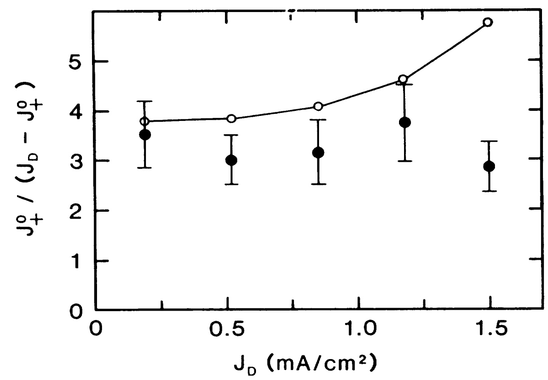

FIG. 3. Ratio of ion to electron current at the cathode, $J_+^0/(J_D - J_+^0)$, as a function of total discharge current density. The experimentally determined values are shown as solid points with a typical uncertainty of $\pm 20\%$. The Monte Carlo results are presented as open circles connected by a line.

charge densities for ions and electrons are nearly equivalent in the negative glow, electrons are carrying the bulk of the current in this region. Ions produced to the right of d_c are lost through recombination and diffusion out of the discharge region.

The empirical ratio of J_+^0 to the electron current density at the cathode, $J_D - J_+^0$, is compared in Fig. 3 to the average number of ions produced in the cathode fall per emitted electron as calculated by use of the Monte Carlo simulation. The ratio is only weakly dependent on cathode-fall voltage due to the gas-density reduction from heating. The Monte Carlo simulations are strongly dependent on gas density. A 6% change in the gas density at high currents (the uncertainty) propagates in the simulation to a 20% change in the average avalanche size as that presented in Fig. 3. The imperfect agreement between theory and experiment at high discharge currents is due to the sensitivity of the Monte Carlo simulations to uncertainties in gas density and electron-impact cross sections ($\pm 25\%$). The good agreement at lower currents gives us confidence that we have determined this critical parameter.

The determination of the current balance at the cathode surface is a significant step toward a detailed quantitative model of the cathode-fall region. Yet to be understood is the relative importance of electron emission from the cathode due to ion, metastable, and uv photon bombardment. Ultimately, a direct Boltzmann equation or nonequilibrium fluid model should be coupled with Poisson's equation to predict both the cathode-fall voltage and the spatial dependence of the field. Such an approach should also be able to predict the existence and properties of the negative glow.

This research is supported by the U.S. Army Research Office and the U.S. Air Force Office of Scientific Research under Grant No. AFOSR-84-0328. We wish to acknowledge many helpful discussions with Dr. A. C. Gallagher.

[1]C. A. Moore, G. P. Davis, and R. A. Gottscho, Phys. Rev. Lett. **52**, 538 (1984).

[2]D. K. Doughty and J. E. Lawler, Appl. Phys. Lett. **45**, 611 (1984).

[3]D. K. Doughty, S. Salih, and J. E. Lawler, Phys. Lett. **103A**, 41 (1984).

[4]J. E. Lawler, Phys. Rev. A **32**, 2977 (1985).

[5]H. R. Skullerud, J. Phys. D **1**, 1567 (1968).

[6]S. L. Lin and J. N. Bardsley, J. Chem. Phys. **66**, 435 (1977).

[7]J. P. Boeuf and E. Marode, J. Phys. D **15**, 2169 (1982).

[8]M. L. Zimmerman, M. G. Littman, M. M. Kash, and D. Kleppner, Phys. Rev. A **20**, 2251 (1979).

[9]B. N. Ganguly, J. Shoemaker, B. L. Preppernau, and A. Garscadden, J. Appl. Phys. (to be published).

[10]W. L. Wiese, M. W. Smith, and B. M. Glennon, in *Atomic Transition Probabilities, Volume I, Hydrogen Through Neon,* U.S. National Bureau of Standards, National Standard Reference Data Series—4 (U.S. GPO, Washington, D.C., 1966), p. 128.

[11]The pressure-broadening coefficient of 42.0 ± 2.7 MHz/Torr at 292 K for the 501.6-nm transition is from J. E. Lawler, Ph.D. thesis, University of Wisconsin, 1978 (unpublished).

[12]H. Helm, J. Phys. B **10**, 3683 (1977).

[13]S. Sinha, S. L. Lin, and J. N. Bardsley, J. Phys. B **12**, 1613 (1979).

[14]G. D. Alkhazov, Zh. Tekh. Fiz. **40**, 97 (1970) [Sov. Phys. Tech. Phys. **15**, 66 (1970)].

[15]R. W. LeBahn and J. Callaway, Phys. Rev. A **2**, 366 (1970).

[16]A. V. Phelps, Phys. Rev. **99**, 1307 (1955).

[17]W. C. Fon, K. A. Berrington, P. G. Burke, and A. E. Kingston, J. Phys. B **14**, 2921 (1981).